Geophysical Research Letters

Supporting Information for

Using a large ensemble of simulations to assess the Northern Hemisphere stratospheric dynamical response to tropical volcanic eruptions and its uncertainty

Matthias Bittner[1,2], Hauke Schmidt[1], Claudia Timmreck[1], Frank Sienz[1]

[1] Max Planck Institute for Meteorology, Hamburg, Germany

[2] International Max Planck Research School on Earth System Modelling (IMPRS), Hamburg, Germany

Contents of this file

Introduction

Text S1 describes the model used in this study (MPI-ESM-LR). Text S2 provides details about the methodology used to obtain the anomalies after volcanic eruptions as well as the minimum ensemble size.
Table S1 includes the tropical volcanic eruptions considered in this study. Table S2 lists the coupled climate models used for the multi-model mean analysis.
Figure S1 shows the NH polar vortex responses to the eruptions of El Chichón, Pinatubo and their average for the individual ensemble members. Also shown is the polar vortex response in the ERA-Interim reanalysis data for the same eruptions.

Text S1: Model description

In this study we use the Max Planck Institute Earth System Model in its configuration referred to as "low resolution" (MPI-ESM-LR) version 1.1. The MPI-ESM-LR consist of an atmospheric model (ECHAM6.3) [*Stevens et al.*, 2013] including a land component (JSBACH3.0) [*Reick et al.*, 2013] coupled to an ocean model (MPIOM1.6) [*Jungclaus et al.*, 2013] including an ocean biogeochemistry component (HAMOCC) [*Ilyina et al.*, 2013]. The horizontal spectral resolution of ECHAM6 in this configuration is T63 (corresponding to approximately 1.9° x 1.9° at the Equator), and the model has 47 vertical layers up to 0.01 hPa. No quasi-biennial oscillation (QBO) is produced in this version of the model. The ocean model has a GR1.5 (i.e. about 1.5° resolution) grid with two poles. In the coupled model intercomparison project 5 (CMIP5), an earlier version of the model was used (MPI-ESM 1.0) and was extensively validated by numerous studies [*Reichler et al.*, 2012; *Cattiaux and Cassou*, 2013; *Charlton-Perez et al.*, 2013; *Giorgetta et al.*, 2013; *Schmidt et al.*, 2013]. A major difference to the CMIP5 version of the MPI-ESM is the implementation of the new release of the atmosphere model (ECHAM6.3). In addition to several bug fixes, a new radiation code is applied in ECHAM6.3 which leads to small changes in the temperature fields. With regard to the middle atmosphere in the NH high latitudes, the MPI-ESM-LR version 1.1 compares well with the previous version of the MPI-ESM described by *Schmidt et al.* [2013].
The 100-member ensemble of historical simulations (1850 – 2005) follows the respective CMIP5 protocol [*Taylor et al.*, 2011] and is forced with the same prescribed changes in natural and anthropogenic parameters as the CMIP5 simulations with the MPI-ESM-LR version 1.1 [*Giorgetta et al.*, 2013]. The anthropogenic forcings include well-mixed greenhouse gases, anthropogenic sulfate aerosols and man-made land use change. Ozone concentrations of the historical simulations are prescribed according to *Cionni et al.* [2011] as monthly zonal mean values which do not include variability related to volcanic aerosols. Volcanic aerosol forcing is prescribed from an extended version of the Pinatubo aerosol data set by *Stenchikov et al.* [1998]. This data set is based on SAGE II satellite measurements of aerosol extinction. The volcanic forcing contains monthly mean zonal averages of aerosol extinction, single scattering albedo and asymmetry factor as a function of wavelength and pressure. The forcing is given at 40 pressure levels, which are interpolated to the hybrid model layers during the simulation. The horizontal resolution is 2° from 89°S to 89°N.

Text S2: Methods

The post-eruption anomalies are calculated as the difference between the first winter (DJF) after the eruption and the mean of a pre-defined reference period. The reference period is selected for each eruption individually and its length is given by the maximum period prior to the eruption which is not perturbed by a preceding eruption (see Table S1). In this way we account for the different climate states before and after the different eruptions. The practice of selecting individual reference periods is widely used [*Stenchikov et al.*, 2006; *Driscoll et al.*, 2012] and we assume that for the short-term stratospheric dynamical response it is justified to combine anomalies based on different background conditions.

We identify the minimum ensemble size needed to obtain a significant response based on a bootstrap method. We first average the variable of interest (NH polar vortex strength, zonal mean zonal wind, zonal mean temperature) over the individual volcanic reference period for each of the 100 ensemble members. In this way we account for the state of the climate system (e.g. the state of the Atlantic Meridional Overturning Circulation or the sea ice cover) which could potentially be important for the volcanic response. We then calculate the anomaly by subtracting the reference mean from the post-eruption year from the same ensemble member (paired test) [*von Storch*, 1999; *Wilks*, 2011]. This test explicitly accounts for the variance in the reference period by taking an estimate of the sample mean. For an ensemble size of 1, we get 100 different responses to a volcanic eruption corresponding to the 100 different ensemble members (see Figure S1 for the strength of the polar vortex after the eruptions of Pinatubo, El Chichón and the average of Pinatubo and El Chichón). For ensemble sizes **n** = 2 to 100, we randomly draw **n** post-eruption anomalies and calculate the ensemble average. We repeat the calculation 5,000 times to obtain a distribution of anomalies for each **n** from 1 to 100. The minimum number of ensemble members needed to identify a significant volcanic response is defined by the **n** where both, the upper (lower) 90% (or 98%) confidence intervals of the anomaly distribution are greater (lower) than zero. In that case, the anomaly averaged over the 5,000 draws is defined as significantly different from zero at the 95% (or 99%) confidence level.

For the multi-model mean response to volcanic eruptions, we use the historical simulations of 15 CMIP5 models (see Table S1). The models have been interpolated to a common grid defined by the lowest vertical (NorESM1-M) and horizontal (HadGEM2-ES) model resolution. To obtain the multi-model mean, we average the ensemble mean of each individual model with equal weight.

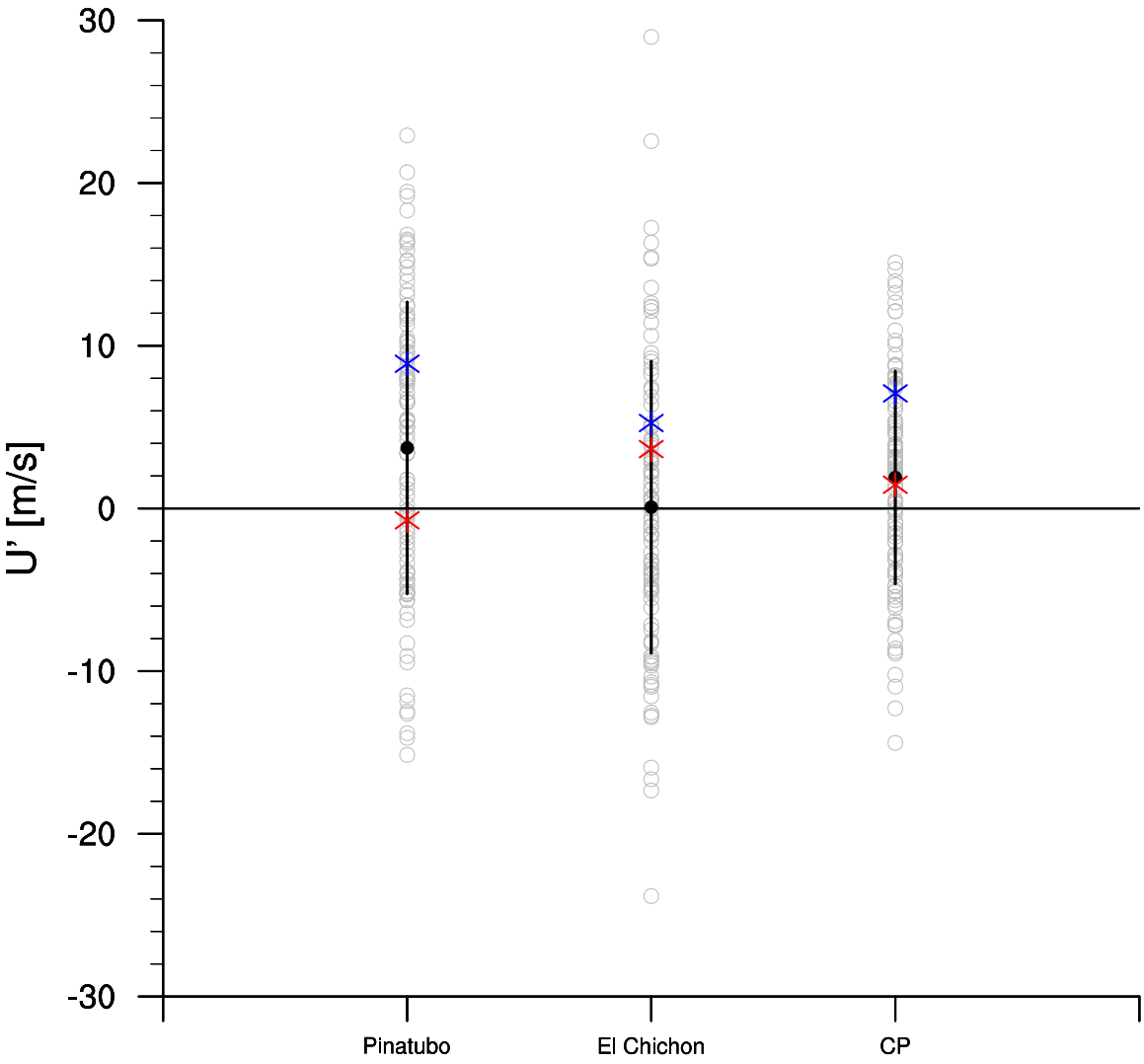

Figure S1. Zonal mean zonal wind anomalies between 55°N – 65°N at 10 hPa (m/s) in the first winter (DJF) following the eruptions of Pinatubo, El Chichón and the average of these two eruptions (CP). Grey circles are the anomalies of the individual ensemble members, the black dots are the ensemble means and the black lines indicate the 1-standard-deviation interval. The stars are the zonal wind anomalies at the same location in the first (red) and second (blue) winter in the ERA-Interim reanalysis data [*Dee et al.*, 2011]. Because ERA-Interim starts in 1979, only three years prior the El Chichón eruption are used as reference years.

	ERUPTION DATE	ERUPTION LATITUDE	WINTER (DJF) ANALYZED	REFERENCE WINTERS (DJF)	TROPICAL AOD / RANK
KRAKATAU	Aug 27,1883	6.10°S	1883/1884	1859/1860-1882/1883	0.182 / 1
TARAWERA	Jun 10,1886	38.23°S	1886/1887	1859/1860-1882/1883	0.055 / 6
BANDAI	Jul 15,1888	36.60°S	1888/1889	1859/1860-1882/1883	0.039 / 7
SANTA MARÍA	Oct 24,1902	14.76°N	1903/1904	1890/1891-1901/1902	0.092 / 4
QUIZAPU	Apr 10,1932	35.65°S	1932/1933	1914/1915-1931/1932	0.008 / 9
AGUNG	Mar 17,1963	9.34°N	1963/1964	1935/1936-1955/1956	0.072 / 5
FUEGO	Oct 10,1974	14.47°N	1975/1976	1966/1967-1973/1974	0.022 / 8
EL CHICHÓN	Apr 4,1982	17.36°N	1982/1983	1977/1978-1981/1982	0.107 / 3
PINATUBO	Jun 15,1991	15.13°N	1991/1992	1985/1986-1990/1991	0.156 / 2

Table S1. The nine strongest, tropical volcanic eruptions since 1880, with post-eruption winters and reference periods as in [*Driscoll et al.*, 2012]. The rank corresponds to their magnitude defined by the tropical (20°N-20°S) Aerosol Optical Depth in the first post-eruption winter (DJF) in the volcanic forcing dataset of *Stenchikov et al.* [1998].

MODEL NAME	MODELLING GROUP	VOLCANIC FORCING	ENSEMBLE SIZE
BCC-CSM1-1[A]	Beijing Climate Center	Ammann 2003	3
CEMS1-CAM5[B]	National Canter for Atmospheric Research	Interactive	3
CANESM2[C]	Candadian Centre for Climate Modelling	Sato	5
CCSM4[D]	National Canter for Atmospheric Research	Ammann 2007	6
CNRM-CM5[E]	Centre National de Recherches Meteorologique	Ammann 2007	10
CSIRO-MK3-6-0[F]	Commonwealth Scientific and Industrial Research Organization	Sato	10
GISS-E2-R[G]	NASA Goddard Institute for Space Science	Sato	6
GFDL-CM3[H]	NOAA Geophysical Fluid Dynamics Laboratory	Stenchikov	5
HADGEM2-ES[I]	Met Office Hadley Centre	Sato	4
MIROC-ESM[J]	Japan Agency for Marine-Earth Science and Technology	Sato	3
MPI-ESM-LR[K]	Max Planck Institute for Meteorology	Stenchikov	10
MPI-ESM-MR[K]	Max Planck Institute for Meteorology	Stenchikov	3
MRI-CGCM3[L]	Meteorological Research Institute	Interactive	5
NORESM1-M[M]	Norwegian Climate Centre	Ammann 2007	3
CESM1-WACCM[N]	National Canter for Atmospheric Research	Interactive	7

Table S2. Models considered in this study for the multi-model mean analysis. The volcanic forcing is based on *Ammann* [2003], its updated version *Ammann et al.* [2007], *Sato et al.* [1993], or *Stenchikov et al.* [1998], respectively. The MRI-CGCM3 computes the conversion of SO_2 amount to stratospheric aerosol with the aerosol module MASINGAR mk-2 [*Tanaka et al.*, 2003]. The CESM1-CAM5 and CESM1-WACCM prescribe surface area density of the volcanic aerosols and calculate heating rates [*Marsh et al.*, 2013]. For the CESM1-WACCM the historical simulation is provided only for the period 1960 – 2005. Hence, only volcanic eruptions after 1960 are considered for this model.

[A] *Wu et al.* [2013]
[B] *Hurrell et al.* [2013]
[C] *Chylek et al.* [2011]
[D] *Gent et al.* [2011]
[E] *Voldoire et al.* [2012]
[F] *Rotstayn et al.* [2010]
[G] *Schmidt et al.* [2014]
[H] *Donner et al.* [2011]
[I] *Collins et al.* [2011]
[J] *Watanabe et al.* [2011]
[K] *Giorgetta et al.* [2013]
[L] *Yukimoto et al.* [2012]
[M] *Bentsen et al.* [2012]
[N] *Marsh et al.* [2013]

References

Ammann, C. M. (2003), A monthly and latitudinally varying volcanic forcing dataset in simulations of 20th century climate, *Geophys. Res. Lett.*, *30*, doi:10.1029/2003GL016875.

Ammann, C. M., F. Joos, D. S. Schimel, B. L. Otto-Bliesner, and R. A. Tomas (2007), Solar influence on climate during the past millennium: results from transient simulations with the NCAR Climate System Model., *Proc. Natl. Acad. Sci. U. S. A.*, *104*, 3713–3718, doi:10.1073/pnas.0605064103.

Bentsen, M. et al. (2012), The Norwegian Earth System Model, NorESM1-M – Part 1: Description and basic evaluation, *Geosci. Model Dev. Discuss.*, *5*(3), 2843–2931, doi:10.5194/gmdd-5-2843-2012.

Cattiaux, J., and C. Cassou (2013), Opposite CMIP3/CMIP5 trends in the wintertime Northern Annular Mode explained by combined local sea ice and remote tropical influences, *Geophys. Res. Lett.*, *40*(14), 3682–3687, doi:10.1002/grl.50643.

Charlton-Perez, A. J. et al. (2013), On the lack of stratospheric dynamical variability in low-top versions of the CMIP5 models, *J. Geophys. Res. Atmos.*, *118*, 2494–2505, doi:10.1002/jgrd.50125.

Chylek, P., J. Li, M. K. Dubey, M. Wang, and G. Lesins (2011), Observed and model simulated 20th century Arctic temperature variability: Canadian Earth System Model CanESM2, *Atmos. Chem. Phys. Discuss.*, *11*(8), 22893–22907, doi:10.5194/acpd-11-22893-2011.

Cionni, I., V. Eyring, J. F. Lamarque, W. J. Randel, D. S. Stevenson, F. Wu, G. E. Bodeker, T. G. Shepherd, D. T. Shindell, and D. W. Waugh (2011), Ozone database in support of CMIP5 simulations: results and corresponding radiative forcing, *Atmos. Chem. Phys.*, *11*(21), 11267–11292, doi:10.5194/acp-11-11267-2011.

Collins, W. et al. (2011), Development and evaluation of an Earth-System model – HadGEM2, *Geosci. Model Dev.*, *4*, 1051–1075, doi:10.5194/gmd-4-1051-2011.

Dee, D. P. et al. (2011), The ERA-Interim reanalysis: Configuration and performance of the data assimilation system, *Q. J. R. Meteorol. Soc.*, *137*(656), 553–597, doi:10.1002/qj.828.

Donner, L. J. et al. (2011), The Dynamical Core, Physical Parameterizations, and Basic Simulation Characteristics of the Atmospheric Component AM3 of the GFDL Global Coupled Model CM3, *J. Clim.*, *24*(13), 3484–3519, doi:10.1175/2011JCLI3955.1.

Driscoll, S., A. Bozzo, L. J. Gray, A. Robock, and G. Stenchikov (2012), Coupled Model Intercomparison Project 5 (CMIP5) simulations of climate following volcanic eruptions, *J. Geophys. Res.*, *117*(D17105), doi:10.1029/2012JD017607.

Gent, P. R. et al. (2011), The Community Climate System Model Version 4, *J. Clim.*, *24*(19), 4973–4991, doi:10.1175/2011JCLI4083.1.

Giorgetta, M. A. et al. (2013), Climate and carbon cycle changes from 1850 to 2100 in MPI-ESM simulations for the coupled model intercomparison project phase 5, *J. Adv. Model. Earth Syst.*, *5*, 572–597, doi:10.1002/jame.20038.

Hurrell, J. W. et al. (2013), The Community Earth System Model: A Framework for Collaborative Research, *Bull. Am. Meteorol. Soc.*, *94*(9), 1339–1360, doi:10.1175/BAMS-D-12-00121.1.

Ilyina, T., K. D. Six, J. Segschneider, E. Maier-Reimer, H. Li, and I. Núñez-Riboni (2013), Global ocean biogeochemistry model HAMOCC: Model architecture and performance as component of the MPI-Earth system model in different CMIP5 experimental realizations, *J. Adv. Model. Earth Syst.*, *5*(2), 287–315, doi:10.1029/2012MS000178.

Jungclaus, J. H., N. Fischer, H. Haak, K. Lohmann, J. Marotzke, D. Matei, U. Mikolajewicz, D. Notz, and J. S. von Storch (2013), Characteristics of the ocean simulations in the Max Planck Institute Ocean Model (MPIOM) the ocean component of the MPI-Earth system model, *J. Adv. Model. Earth Syst.*, *5*(2), 422–446, doi:10.1002/jame.20023.

Marsh, D. R., M. J. Mills, D. E. Kinnison, J.-F. Lamarque, N. Calvo, and L. M. Polvani (2013), Climate Change from 1850 to 2005 Simulated in CESM1(WACCM), *J. Clim.*, *26*(19), 7372–7391, doi:10.1175/JCLI-D-12-00558.1.

Reichler, T., J. Kim, E. Manzini, and J. Kroger (2012), A stratospheric connection to Atlantic climate variability, *Nat. Geosci*, *5*(11), 783–787, doi:10.1038/ngeo1586.

Reick, C. H., T. Raddatz, V. Brovkin, and V. Gayler (2013), Representation of natural and anthropogenic land cover change in MPI-ESM, *J. Adv. Model. Earth Syst.*, *5*(3), 459–482, doi:10.1002/jame.20022.

Rotstayn, L. D., M. A. Collier, M. R. Dix, Y. Feng, H. B. Gordon, S. P. O'Farrell, I. N. Smith, and J. Syktus (2010), Improved simulation of Australian climate and ENSO-related rainfall variability in a global climate model with an interactive aerosol treatment, *Int. J. Climatol.*, *30*(7), 1067–1088, doi:10.1002/joc.1952.

Sato, M., J. E. Hansen, M. P. McCormick, and J. B. Pollack (1993), Stratospheric aerosol optical depths, 1850–1990, *J. Geophys. Res. Atmos.*, *98*(D12), 22987–22994, doi:10.1029/93JD02553.

Schmidt, G. A. et al. (2014), Configuration and assessment of the GISS ModelE2 contributions to the CMIP5 archive, *J. Adv. Model. Earth Syst.*, *6*(1), 141–184, doi:10.1002/2013MS000265.

Schmidt, H. et al. (2013), Response of the middle atmosphere to anthropogenic and natural forcings in the CMIP5 simulations with the Max Planck Institute Earth system model, *J. Adv. Model. Earth Syst.*, *5*(1), 98–116, doi:10.1002/jame.20014.

Stenchikov, G., K. Hamilton, R. J. Stouffer, A. Robock, V. Ramaswamy, B. Santer, and H.-F. Graf (2006), Arctic Oscillation response to volcanic eruptions in the IPCC AR4 climate models, *J. Geophys. Res.*, *111*(D7), D07107, doi:10.1029/2005JD006286.

Stenchikov, G. L., I. Kirchner, A. Robock, H.-F. Graf, J. C. Antuña, R. G. Grainger, A. Lambert, and L. Thomason (1998), Radiative forcing from the 1991 Mount Pinatubo volcanic eruption, *J. Geophys. Res.*, *103*(D12), 13837–13857, doi:10.1029/98JD00693.

Stevens, B. et al. (2013), Atmospheric component of the MPI-M Earth System Model: ECHAM6, *J. Adv. Model. Earth Syst.*, *5*(2), 146–172, doi:10.1002/jame.20015.

von Storch, H. (1999), Misuses of Statistical Analysis in Climate Research, in *Analysis of Climate Variability*, pp. 11–26, Springer Berlin Heidelberg, Berlin, Heidelberg.

Tanaka, T. Y., K. Orito, T. T. Sekiyama, K. Shibata, M. Chiba, and H. Tanaka (2003), MASINGAR, a global tropospheric aerosol chemical transport model coupled with MRI/JMA98 GCM, *Pap. Meteorol. Geophys.*, *53*(4), 119–138, doi:10.2467/mripapers.53.119.

Taylor, K. E., R. J. Stouffer, and G. A. Meehl (2011), An Overview of CMIP5 and the Experiment Design, *Bull. Amer. Meteor. Soc.*, *93*(4), 485–498, doi:10.1175/BAMS-D-11-00094.1.

Voldoire, A. et al. (2012), The CNRM-CM5.1 global climate model: description and basic evaluation, *Clim. Dyn.*, *40*(9-10), 2091–2121, doi:10.1007/s00382-011-1259-y.

Watanabe, S. et al. (2011), MIROC-ESM 2010: model description and basic results of CMIP5-20c3m experiments, *Geosci. Model Dev.*, *4*(4), 845–872, doi:10.5194/gmd-4-845-2011.

Wilks, D. S. (2011), *Statistical Methods in the Atmospheric Sciences*, 3rd ed., International Geophysics, Elsevier, Amsterdam, The Netherlands.

Wu, T. et al. (2013), Global carbon budgets simulated by the Beijing Climate Center Climate System Model for the last century, *J. Geophys. Res. Atmos.*, *118*(10), 4326–4347, doi:10.1002/jgrd.50320.

Yukimoto, S. et al. (2012), A New Global Climate Model of the Meteorological Research Institute: MRI-CGCM3 ^|^mdash;Model Description and Basic Performance^|^mdash;, *J. Meteorol. Soc. Japan*, *90A*, 23–64, doi:10.2151/jmsj.2012-A02.